

## Crustal displacements due to continental water loading

T. van Dam,<sup>1</sup> J. Wahr,<sup>2</sup> P. C. D. Milly,<sup>3,4</sup> A. B. Shmakin,<sup>4,5</sup> G. Blewitt,<sup>6,7</sup>  
D. Lavallée,<sup>8</sup> and K. M. Larson<sup>9</sup>

**Abstract.** The effects of long-wavelength ( $> 100$  km), seasonal variability in continental water storage on vertical crustal motions are assessed. The modeled vertical displacements ( $\Delta r_M$ ) have root-mean-square (RMS) values for 1994-1998 as large as 8 mm, with ranges up to 30 mm, and are predominantly annual in character. Regional strains are on the order of 20 nanostrain for tilt and 5 nanostrain for horizontal deformation. We compare  $\Delta r_M$  with observed Global Positioning System (GPS) heights ( $\Delta r_O$ ) (which include adjustments to remove estimated effects of atmospheric pressure and annual tidal and non-tidal ocean loading) for 147 globally distributed sites. When the  $\Delta r_O$  time series are adjusted by  $\Delta r_M$ , their variances are reduced, on average, by an amount equal to the variance of the  $\Delta r_M$ . Of the  $\Delta r_O$  time series exhibiting a strong annual signal, more than half are found to have an annual harmonic that is in phase and of comparable amplitude with the annual harmonic in the  $\Delta r_M$ . The  $\Delta r_M$  time series exhibit long-period variations that could be mistaken for secular tectonic trends or post-glacial rebound when observed over a time span of a few years.

## Introduction

The positioning time series from an individual GPS site commonly contains a significant displacement associated with the response of the earth to surface mass loading [van Dam and Wahr, 1998]. Among the loads likely to be important are those due to changes in atmospheric pressure, to tidal and non-tidal fluctuations in the ocean, and to variations in the distribution of water, snow, and ice on land. Of these, the effects of large-scale terrestrial water storage are the least well understood; their quantification is the purpose of this analysis. We use a model of global continental water-storage variations, together with a model of how the earth deforms in response to a surface load, to

predict vertical crustal motions due to long-wavelength ( $> 100$  km) loading by continental water storage. We compare the modeled vertical surface displacements ( $\Delta r_M$ ) with monthly height estimates from 147 globally distributed GPS sites. We also estimate the contribution of low-frequency variations in continental water loading to observed vertical displacement trends.

## Calculation of continental water-storage loading and response

Storage of water in snowpack, soil, and groundwater was calculated using a global model of land water and energy balance, on a  $1^\circ$ -by- $1^\circ$  grid. The model is forced by estimated precipitation, downwelling radiation, and near-surface atmospheric conditions. Snowpack is tracked as a single store using mass- and energy-balance accounting. Snowmelt and rainfall recharge a single soil-water store until it is full (i.e., reaches field capacity), at which point any excess water recharges groundwater. Groundwater discharges to surface water at a rate proportional to groundwater storage, and surface-water storage changes are assumed negligible. Evaporation depletes snowpack at a rate determined by energy availability. Elsewhere, evaporation removes water from the soil at a rate determined by energy and water availability. Anthropogenic groundwater mining and surface-water impoundments are ignored, though these can have substantial local effects on storage and resultant loading. Ice-flow dynamics are not modeled, so modeled mass changes are not physically realistic for ice sheets and glaciers. Model parameters are estimated from global maps of biome types and soil texture. Forcing is synthesized from the International Satellite Land Surface Climatology Project (ISLSCP) Initiative I dataset [Meeson *et al.*, 1995], the Global Historical Climatology Network precipitation records, and the Climate Prediction Center (CPC) Merged Analysis of Precipitation (CMAP) [Xie and Arkin, 1977]. The model simulated the period 1979-1998.

Considerable errors are probably present in the model-derived water-storage estimates. These arise from errors in forcing, parameters, and model formulation. However, we expect that the model will tend to reproduce the temporal and spatial structure of storage reasonably well [Shmakin and Milly, 1999].

Summation of model storage outputs (snow, soil water and groundwater) provides our estimate of terrestrial water storage loading on a monthly time scale. Here we focus on results for 1994-1998. Because of the noted limitation of the model in areas of permanent ice cover, calculated snow storage is ignored in Greenland, Antarctica and other glaciated grid cells. At most locations, we find the load is dominated by an annually-varying signal. Over tropical areas in Africa and South America, and in the region of the Asian monsoon, the range (maximum-minimum) of water-storage load

<sup>1</sup>Luxembourg National Museum of Natural History and the European Center for Geodynamics and Seismology, Walferdange, Luxembourg.

<sup>2</sup>Department of Physics and CIRES, University of Colorado, Boulder, Colorado.

<sup>3</sup>U.S. Geological Survey, Princeton, New Jersey.

<sup>4</sup>Geophysical Fluid Dynamics Laboratory/NOAA, Princeton, New Jersey.

<sup>5</sup>Now at the Institute of Geography, Russian Academy of Sciences, Moscow.

<sup>6</sup>Nevada Bureau of Mines and Geology, Reno, Nevada.

<sup>7</sup>Seismological Laboratory, University of Nevada, Reno.

<sup>8</sup>Department of Geomatics, University of Newcastle upon Tyne, England.

<sup>9</sup>Department of Aerospace Engineering, University of Colorado, Boulder, Colorado.

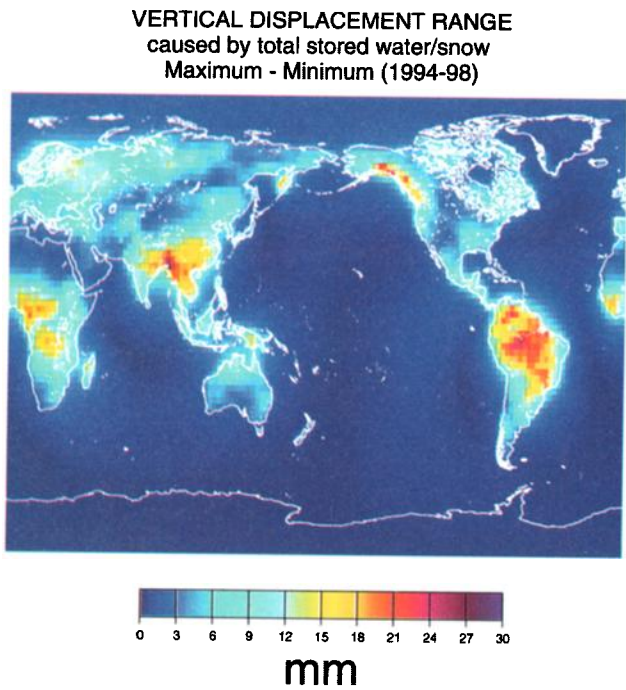


**Figure 1.** Maximum range in vertical crustal displacement during 1994-1998 (mm) due to changes in total continental water storage.

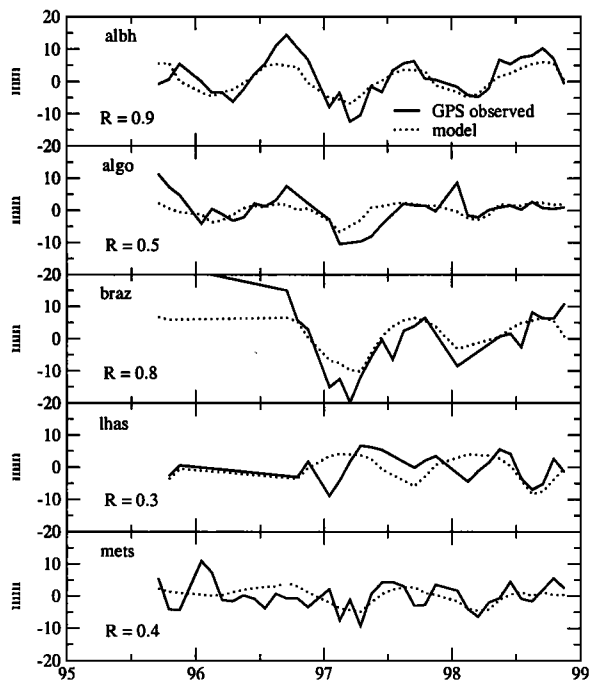


**Figure 2.** Modeled maximum water-storage-induced vertical displacements ( $\Delta r_M$ , mm) at selected GPS locations (dotted lines) and monthly averages of GPS height residuals ( $\Delta r_O$ , mm) after atmospheric pressure and nontidal and tidal annually varying loading corrections (solid lines). Victoria (albh), in Western Canada; Algonquin Park (algo), in Eastern Canada; Brasilia, Brazil (braz); Lhasa, China (lhas) on the Tibetan Plateau; and Kirkkonummi, Finland (mets). The R values represent the amplitudes of the correlations between the two signals.

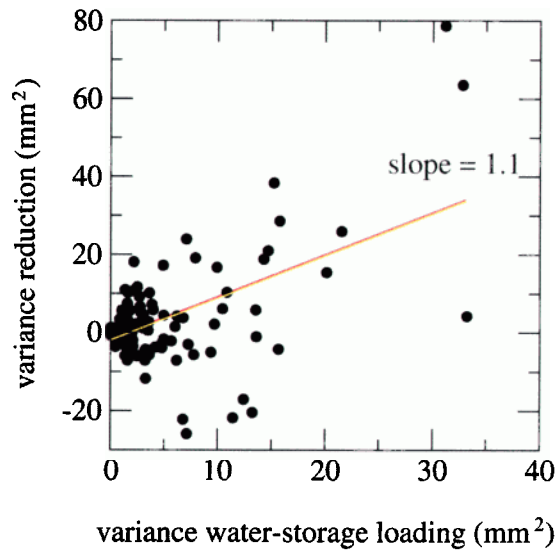


**Figure 3.** Reduction in variance of GPS height residuals due to adjustment by  $\Delta r_M$ . ( $\text{Var}[\Delta r_O] - \text{Var}[\Delta r_O - \Delta r_M]$ ),  $\text{mm}^2$ , plotted as a function of the  $\text{Var}[\Delta r_M]$ ,  $\text{mm}^2$ . Each symbol represents one GPS site. The slope, with a standard error of 0.14, does not differ significantly from 1, but differs significantly from 0.

can be between 500 and 1000 mm. Variations between 1000 and 2000 mm are observed along the western coast of North America, extending from Alaska into northern California. The RMS value of the load tends to be about one-fourth of the full load range, consistent with the load being dominantly seasonal but having significant interannual variability in amplitude.

Estimates of the vertical surface displacements ( $\Delta r_M$ ) are calculated by convolving *Farrell's* [1972] Greens functions with the surface load. In Figure 1, we map the full modeled range of  $\Delta r_M$ . In the Asian monsoon region, in tropical South America and Africa, and along the western coast of Canada and the southern coast of Alaska, the  $\Delta r_M$  can be

### TRENDS 1996-1998

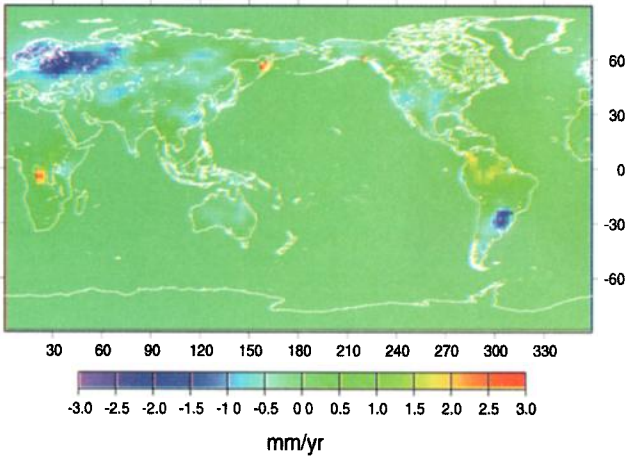


**Figure 4.** Global distribution of vertical displacement rates (mm/yr) modeled using 3 years (1996-1998) of water-storage data.

as large as 30 mm. Over most of the continental areas, however, the expected ranges are between 9 and 15 mm. (Horizontal displacements are much smaller, with maximum variations of about 5 mm in those areas noted as having a large vertical signal.) Resultant upper-bound strains are 20 mm/1000 km or 20 nanostrain for tilt, 5 mm/1000 km or 5 nanostrain for horizontal deformation. In general, the map of the RMS values of  $\Delta r_M$  (not shown) resembles that of the  $\Delta r_M$  range, but reduced in magnitude by a factor of about 4.

The dotted lines in Figure 2 show time series of  $\Delta r_M$  for some GPS sites. Each station  $\Delta r_M$  in the figure has a loading signal range of 20 to 30 mm. The signal is strongly annual in character, but with an annual amplitude that can vary significantly from year to year.

## Comparison with GPS height residuals

Our estimates of  $\Delta r_M$  are the same order of magnitude as typical variations observed in GPS vertical positioning. Here we compare  $\Delta r_M$  with height residuals obtained from GPS weekly Solution Independent Exchange (SINEX) format combination files [Davies and Blewitt, 2000] at 147 globally distributed GPS sites.

The GPS time series represent residuals after estimating a 6-parameter Helmert transformation (no scale) between epoch solutions and mapped epoch solutions from a kinematic free-network combination [van Dam et al., 1994]. Note the specific choice of reference frame and ellipsoid definition is inconsequential for our purposes. We are only interested in height variations, which are no larger than a few centimeters, and are thus insensitive to the definition of the local vertical direction.

Even though the process of frame alignment does not affect internal geometry, it has been shown that it can dampen signals in individual coordinate time series. Blewitt and Lavallée [2000] show evidence for this effect for global-scale seasonal signals, producing a spurious latitude-dependent seasonal signal at the 1 mm level. As we are analyzing signals of this nature, our time series might be systematically affected at this level.

Estimated weekly-averaged atmospheric loading effects [van Dam et al., 1994], and the effects of tidal and non-tidal annually-varying oceanic loading [van Dam et al., 1997] are first removed from these SINEX combination files. (Note: Diurnal, semi-diurnal, semi-monthly, monthly, and semi-annual tidal ocean loading effects have already been removed by the International GPS Analysis Centers prior to combination.) Annual tidal and non-tidal ocean loading effects are small with amplitudes of usually less than 2 mm. For the remainder of this paper the term residuals will refer to the SINEX heights with these loading effects removed.

The weekly residuals are then averaged into monthly estimates that correspond to the epochs of the water-storage data. The resulting GPS-derived displacement time series ( $\Delta r_O$ ) range in length from 6 months to 36 months and have RMS scatter ranging from 2.2 to 15.8 mm. In comparison, the RMS value of  $\Delta r_M$  for these sites varies from about 0.1 to 5.8 mm. Therefore, we do not expect continental water loading to explain fully the adjusted GPS height residuals.

In Figure 2, we superimpose the  $\Delta r_M$  onto the  $\Delta r_O$  time series for the GPS sites selected. The  $\Delta r_M$  track the  $\Delta r_O$  reasonably well at all of these sites, demonstrating that

water-storage loading may indeed be the cause of some of the long-period variability which is observed in GPS time series from locations where the water-storage loading effect is large.

We computed the variances of  $\Delta r_O$  and  $\Delta r_O - \Delta r_M$ , and the difference between these variances. If the  $\Delta r_M$  were an error-free estimate of the displacement induced by continental water loading and if variance estimates were computed with an infinite number of measurements, then the difference between variances of  $\Delta r_O$  and  $\Delta r_O - \Delta r_M$  would equal the variance of the  $\Delta r_M$ . However, in practice this is not the case due to errors in the model of water storage, due to noise in the GPS residuals, and because our statistics were computed with a finite sample size. Of the 147 time series examined, the variance of 92 of the time series are reduced when we remove the water-storage loading effects. In Figure 3, we show the variance reduction  $\text{Var}[\Delta r_O] - \text{Var}[\Delta r_O - \Delta r_M]$  as a function of the variance of the  $\Delta r_M$  at each GPS site. Despite the considerable scatter, the least-squares linear fit to the data has a slope close to one with a near-zero intercept, indicating that the variance reduction is, on average, approximately equal to the variance of the  $\Delta r_M$ .

We estimated the phase of the annual signal for each time series, using the weekly SINEX files with the estimated pressure-loading and ocean loading (tidal and non-tidal) effects removed. These time series are in general longer and denser than the monthly averages, and thus allow more precision in estimating the phase. Of the 147 time series, 34 have a strong annual signal with a significance greater than .001 [Press and Teukolsky, 1988]. Of this subset, 23 have an annual phase that differs by less than  $\pm 35^\circ$  from the annual phase of the  $\Delta r_M$ . The amplitude of the annual harmonic in the  $\Delta r_M$  for these 23 sites is 25-100% of the amplitude of the annual harmonic in  $\Delta r_O$ . These results indicate that the surface displacements from annual water-storage variations contribute to the annual signal at a significant number of continuous GPS sites.

## Secular trends

Continuous geodetic measurements from a permanent GPS installation would average out most of the water-storage-induced variability after a few years. But because the storage loading contains power at very long periods, some residual linear trend will be present in the GPS measurements, and that trend would be indistinguishable from a secular tectonic trend. Figure 4 shows the inferred linear trend in vertical uplift that would be obtained using the  $\Delta r_M$  from 1996-98. Although the trend is small (less than 0.5 mm/yr) in most regions, the trend is larger than 1 mm/yr in some regions of South America, southern Africa, and the Kamchatka peninsula, with a maximum trend of greater than 2 mm/yr. Regional secular strain rates are usually less than 1 nanostrain/yr. Local effects are not addressed by this study.

The apparent trend caused by water-storage loading decreases as the length of the observing period increases; the trend decreases at all sites from greater than 5 mm/yr after 1 year of data to less than 0.3 mm/yr after 20 years.

## Summary

In this paper we have modeled monthly, global variations of continental water storage and resultant crustal dis-

placements. We conclude that continental water loading can cause vertical displacements of 15 mm or more over large regions of the globe, with displacements of up to 30 mm in some regions. The RMS variability of the displacements can be as large as 8 mm.

GPS height residuals (adjusted for atmospheric pressure and ocean tidal and non-tidal effects loading) routinely exhibit non-secular variability that tends, in fact, to be on the same order as the water-storage effects found here. Some of this observed variability can reflect systematic errors, such as those due to orbit and atmospheric propagation errors. But some of this non-secular variability can also represent real geophysical signals, particularly those caused by variable surface loads. When GPS height residuals are adjusted by the modeled displacements, their variances are reduced, on average, by an amount equal to the variance of the modeled displacements. For SINEX time series with a strong annual signal, the phase of the annual signal in the GPS height residuals differs by less than  $\pm 35^\circ$  from the modeled displacements induced by water-storage variations.

Water-mass loading can include long-term variability, which produces an apparent secular signal over observing periods of a few years. Although these trends tend to be small at most locations (usually less than 0.5 mm/yr over a three-year period), the three-year trend can be as large as 2.5 mm/yr in some regions.

We estimate that upper-bound strains are 20 nanostrain for tilt and 5 nanostrains for horizontal deformation, with secular regional strain rates usually less than 1 nanostrain/yr.

**Acknowledgments.** This work was supported in part by NASA grants NAG5-6147 and NAG5-7703 to the University of Colorado, by NASA's Water Cycle Processes Program through the University Corporation for Atmospheric Research, a NASA grant to the University of Reno, a NREC grant to the University of Newcastle, and a Department of Energy grant "Geodetic Monitoring of the Yucca Mountain Region using Continuous GPS Measurements". K. A. Dunne, D. L. Galloway, and S. Nerem gave us helpful reviews of the manuscript.

## References

- Blewitt, G. and D. Lavallée, Effect of annually repeating signals on geodetic velocity estimates, paper presented at The Tenth General Assembly of the WEGENER Project (WEGENER 2000), San Fernando, Spain, September 18-20, 2000.
- Davies, P. B., and G. Blewitt, Methodology for global geodetic time series estimation: A new tool for geodynamics, *J. Geophys. Res.*, 105, 11,083-11,100, 2000.
- Farrell, W. E., Deformation of the earth by surface loads, *Rev. of Geophys.*, 10, 761-797, 1972.
- Meeson, B. W., F.E. Corprew, J. M. P. McManus, D. M. Myers, J. W. Closs, K.-J. Sun, D. J. Sunday, P. J. Sellers, SLSCP Initiative I-Global data sets for land-atmosphere models, 1987-1988, *Volumes 1-5, Published on CD by NASA USA\_NASA\_GDAAC-ISLSCP.001-USA\_NASA\_GDAAC-ISLSCP.005*, 1995.
- Press, W. H., and A. Teukolsky, Search algorithm for weak signals in unevenly spaced data, *Computers in Physics*, 3, 77-82, 1988.
- Shmakin, A. B., and P. C. D. Milly, Evaluation of interannual variations in runoff from large river basins (abstract), *IUGG XXII General Assembly, Abstracts*, 36, 1999.
- van Dam, T. M., and J. M. Wahr, Modeling environmental loading effects: a Review, *Phys. Chem. Earth*, 23, 1077-1086, 1998.
- van Dam, T. M., J. Wahr, Y. Chao, and E. Leuliette, Predictions of crustal deformation and of geoid and sea-level variability caused by oceanic and atmospheric loading *Geophys. J. Int.*, 99, 507-517, 1997.
- van Dam, T. M., G. Blewitt, and M. Heflin, Detection of atmospheric pressure loading using the Global Positioning System, *J. Geophys. Res.*, 99, 23,939-23,950, 1994.
- Xie, P., and P. A. Arkin, Global precipitation: a 17-year monthly analysis based on gauge observations, satellite estimates, and numerical model outputs, *Bull. Amer. Meteor. Soc.*, 78, 2539-2558, 1997.
- T. van Dam, Luxembourg National Museum for Natural History and the European Center for Geodynamics and Seismology, 19 Rue Josy Welter, L-7256 Walferdange Luxembourg, (e-mail: tonie@ecgs.lu).
- J. Wahr, Department of Physics and CIRES, University of Colorado, Campus Box 216, Boulder, CO 80309, (e-mail: wahr@lemond.colorado.edu).
- P. C. D. Milly, U.S. Geological Survey, GFDL/NOAA, P.O. Box 308, Princeton, NJ, 08542, (e-mail: pcm@gfdl.gov).
- A. B. Shmakin, GFDL/NOAA, (Now at the Institute of Geography, Russian Academy of Sciences, Moscow), (e-mail: cli mate@igras.geonet.ru).
- G. Blewitt, Nevada Bureau of Mines and Geology and Seismological Laboratory, University of Nevada, Reno Mail Stop 178, Reno, NV 89557-0088, (e-mail: gblewitt@unr.edu).
- D. Lavallée, Department of Geomatics, University of Newcastle upon Tyne, Newcastle upon Tyne, NE1 7RU, England, (e-mail: d.a.lavallee@ncl.ac.uk).
- K. M. Larson Department of Aerospace Engineering, University of Colorado, Campus Box 429 ,Boulder, CO, 80309, (e-mail: kristine@brennan.colorado.edu).

(Received July 27, 2000; revised October 30, 2000; accepted November 7, 2000.)